Phys Chem Minerals (2006) 33:691–698
DOI 10.1007/s00269-006-0118-6

ORIGINAL PAPER

Composition, lattice parameters, and room temperature elastic constants of natural single crystal xenotime from Novo Horizonte

P. Mogilevsky · E. B. Zaretsky · T. A. Parthasarathy · F. Meisenkothen

Received: 23 June 2006 / Accepted: 4 October 2006 / Published online: 3 November 2006

Abstract The composition, lattice parameters, and elastic constants of natural single crystal YPO_4 xenotime from Novo Horizonte (Brazil) were determined using EPMA, XRD, and the pulse-echo technique. The composition indicates a 24% substitution of *Y* sites with other rare-earth elements. The lattice parameters of the studied crystal deviated only slightly from those reported for synthetic YPO_4 and were in a good agreement with trends obeyed by other orthophosphates with the xenotime structure. The measured elastic constants C_{11}, C_{33}, C_{44}, and C_{66} were consistent with synthetic crystals when porosity was accounted for. C_{12} and C_{13} constants were evaluated based on the comparison with other materials with xenotime structure. The elastic constants could be rationalized using interionic force constants and bond energies.

Keywords Elastic constants · Composition · Lattice parameters · Fiber reinforced CMCs

Introduction

The co-existence of alumina and monazite in natural minerals served as clue to the identification, development, and use of monazite as an interlayer in high temperature oxide–oxide composites (Davis et al. 1993, 1998; Kerans et al. 2002; Morgan and Marshall 1993, 1995; Morgan et al. 1995; Marshall et al. 1998; Keller et al. 2003). It is now recognized that materials with ABO_4 structure, such as monazite ($LaPO_4$), scheelite ($CaWO_4$), and xenotime (YPO_4) show considerable promise for use as fiber-matrix interlayers in all-oxide ceramic composites. Similar to monazite and scheelite, xenotime (YPO_4) is chemically stable with common structural oxides and bonds weakly to them. However, it has a lower coefficient of thermal expansion (CTE) which may make it a better fiber coating for low thermal expansion fibers. The elastic, plastic, and fracture properties of xenotime will be important in the design of CMCs with these fiber-matrix interlayers. Elastic moduli are also required for the analysis of data that relate to mechanical behavior of these anisotropic materials.

In addition to the prospective applications in all-oxide CMCs, xenotime is also of interest in geological research. Several studies have focused on monazite/xenotime thermobarometry (Gratz and Heinrich 1997, 1998; Andrehs and Heinrich 1998; Pile et al. 2001; Seydoux-Guillaume et al. 2002). Composition of minerals such as xenotime can lead to information about the composition of the parent liquid, provided the partition coefficients are known (Finch et al. 2001). Those, in turn, can be predicted based on the elastic modulus of the mineral (Wood and Blundy 1997; Blundy and Wood 2002, 2003).

Xenotime has a tetragonal structure (space group $I4_1/amd$) with six independent elastic constants. Perfect (100) cleavage has been reported (Roberts et al. 1990). Natural xenotime has Mohs hardness of 4–5 (Roberts

P. Mogilevsky (✉) · T. A. Parthasarathy · F. Meisenkothen
UES Inc., 4401 Dayton-Xenia Rd., Dayton, OH 45432, USA
e-mail: pavel.mogilevsky@wpafb.af.mil

E. B. Zaretsky
Department of Mechanical Engineering, Ben Gurion University of the Negev, Beer-Sheva 84105, Israel

et al. 1990), which corresponds approximately to H_v = 3.1–5.2 GPa (Tabor 1970). Vibration frequencies of synthetic single crystal YPO_4 were determined from an infrared reflection study (Armbruster 1976). The present paper reports on the composition, lattice parameters and elastic constants of natural single crystal xenotime from Novo Horizonte, Brazil.

Experiments

Natural single crystal xenotime ~3 × 1 × 0.8 cm in size (Fig. 1) from Novo Horizonte (Brazil) was supplied by Dr. R. Lavinsky (Arkenstone, Garland, TX). The composition of the crystal was determined using Electron Probe Microanalysis (EPMA, Cameca SX-100). Specific gravity was determined using the Archimedes method. The lattice parameters were determined by X-ray diffraction (XRD, Rigaku Dmax/B rotating anode, Cu–Kα radiation). For lattice parameters measurement, a small piece was cut from the crystal and crushed.

Longitudinal and transverse sound velocity along the three lattice directions *a*, *b*, and *c* was measured using pulse-echo technique with 5-MHz longitudinal and transversal gauges. The ultrasonic measurements were conducted on a rectangular parallelepiped sample cut from the crystal. The opposite sides of sample were ground parallel and polished using a tripod polisher. The polished sample was 8.12 mm along the *c*-axis, 7.43 mm along the *b*-axis, and 7.54 mm along the *a*-axis. The crystallographic orientation of the polished sides of the specimen was verified to be within 1–2° of the corresponding crystallographic directions using XRD.

Experimental results

Composition and density

EPMA revealed the presence of a number of rare earth elements in addition to Y, P, and O. The mean and standard deviation values of 98 point measurements are given in Table 1. Due to the oxygen–yttrium peak overlap, oxygen content was calculated by difference.

The total content of rare earth impurities is 3.99 At.% (Table 1), which is equivalent to ~24% substitution of the *Y* sites. The molar weight is M = 201.486 g/mol, noticeably higher than for pure YPO_4 (M = 183.877 g/mol). Given the structure of xenotime which contains four chemical units per crystal unit cell (Ni et al. 1995), the lattice parameters, and the measured molar weight, the calculated X-ray density of the mineral is 4.658 g/cm^3, higher than 4.26 g/cm^3 for pure YPO_4 (Ni et al. 1995). The actual density measured by Archimedes method is p = 4.547 g/cm^3, which corresponds to ~2.4% total porosity with respect to the calculated density.

Lattice parameters

The long dimension of the crystal corresponded to the *c*-axis, and the large faces were {100} planes. Similar morphologies have been reported for synthetic phosphates, arsenates, and vanadates of Lu and Y (Armbruster 1976) and $ErVO_4$ (Hirano et al. 2002), which belong to the same crystal family. Smaller facets at the tip of the crystal (Fig. 1) were {301} and {101} type.

The XRD spectrum was consistent with the xenotime structure with a strong (100) preferred orientation of the powder particles. This is indicative of easy cleavage on {100}. The lattice parameters obtained from the spectrum were a = 6.8982 ± 0.0001 Å and c = 6.037 ± 0.002 Å [the higher precision in determination of the parameter a is due to the strong (100) preferred orientation in the XRD spectrum]. These are compared with data for natural xenotime from southeast China (Ni et al. 1995) and synthetic YPO_4 (Aldred 1984; Ushakov et al. 2001) in Table 2. The lattice parameters are somewhat larger than those of synthetic pure YPO_4 xenotime (Aldred 1984; Ushakov et al. 2001), and closer to that of natural xenotime from southeast China (Ni et al. 1995).

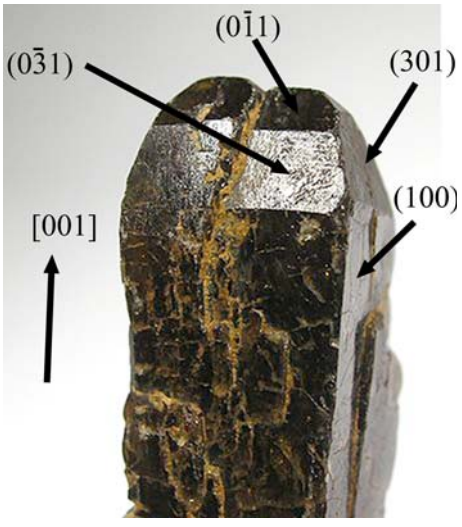

Fig. 1 Xenotime crystal used in this work (original photograph courtesy of Dr. R. Lavinsky, Arkenstone)

Table 1 Composition of the xenotime crystal used in this work (EPMA)

Element	P	O	Y	Rare earth elements									
				Sm	Eu	Gd	Tb	Dy	Ho	Er	Yb	Lu	Σ RE
At.%	16.29	66.86	12.87	0.19	0.12	0.80	0.18	1.40	0.1	0.67	0.35	0.18	3.99
σ	0.13	0.27	0.11	0.01	0.01	0.02	0.01	0.01	0.02	0.01	0.01	0.01	0.11

Table 2 Comparison of measured lattice parameters with those from a mineral from Southeast China and synthetic YPO_4

Mineral source	a (Å)	c (Å)	Reference
Novo Horizonte, Brazil	6.8982 ± 0.0001	6.037 ± 0.002	This work
Southeast China	6.8951	6.0267	Ni et al. (1995)
Synthetic YPO_4	6.8832	6.0208	Ushakov et al. (2001)
	6.884	6.0202	Aldred (1984)

Elastic constants

Pulse-echo measurements along the crystallographic directions *a*, *b*, and *c* were attempted, but reliable measurements were not possible in all directions. Only in the *c*-direction reproducible measurements were obtained. Measurements along the *a* and *b* crystallographic directions were hindered by very high attenuation and multiple reflections from internal interfaces. This is consistent with the reported easy cleavage on {100} planes (Roberts et al. 1990). Indeed, numerous (100) and (010) microcracks were present on a polished (001) cross-section of the sample. These microcracks did not affect the measurements for [001] wave propagation, but did cause high attenuation and reflection from internal interfaces for [100] and [010] directions. As a result, reliable data for *a* and *b* directions were limited to just one measurement for each of these directions. No measurements were attempted in <110> directions, because both (100) and (010) microcracks would interfere with the measurements in these directions.

A summary of the ultrasonic velocities along different directions and the respective elastic constants is shown in Table 3. The uncertainties (where indicated) correspond to the 95% confidence level interval based on 7–8 measurements, except for the [100]/[010] mode where only three successful measurements were obtained. Only one successful velocity measurement was obtained for [010]/[100] and [010]/[001] modes (representing C_{66} and C_{44} constants respectively), and the velocities of [100]/[001] shear and [010]/[010] longitudinal waves could not be measured at all.

In addition to the uncertainty associated with the scatter of the measured ultrasonic velocities, imperfect crystallographic orientation of the sample also contributes to the error in the determination of the elastic constants. Typically, orientation of the specimen surfaces with respect to the lattice vectors within a fraction of 1° is recommended for elastic constants determination (McSkimin 1964), while in this study the specimen was only oriented within 2° of the lattice vectors. However, analysis of the possible effect of the deviation from the precise sample orientation on the measured elastic constants (the effect of rotation of the coordinate system on the stiffness coefficients) indicates that for C_{11}, C_{33}, C_{44}, and C_{13} the rotations of 2° would cause less then 0.2% error. For C_{12} and C_{66} the corresponding errors are 0.6 and 2.2%, respectively. As can be seen from Table 3, for some of the constants, multiple measurements were made. Instead of averaging them, the constants were assigned those values that were deemed most reproducible. The assigned values are underlined in Table 3.

Table 3 Room temperature ultrasonic velocities and elastic constants of natural xenotime

Wave propagation direction	Polarization	Measured ultrasonic velocity (m/s)	Velocity–elastic constant relation	Elastic constant (Gpa)
[100]	[100]	6,960 ± 270	$C_{11} = \rho v^2_{11}$	220.3 ± 17
	[010]	1,950 ± 26	$C_{66} = \rho v^2_{12}$	17.3 ± 0.5
	[001]	–	$C_{44} = \rho v^2_{13}$	–
[010]	[010]	–	$C_{11} = \rho v^2_{22}$	–
	[100]	1,790[a]	$C_{66} = \rho v^2_{21}$	14.6
	[001]	3,700[a]	$C_{44} = \rho v^2_{23}$	62.3
[001]	[001]	8,550 ± 85	$C_{33} = \rho v^2_{33}$	332.4 ± 7
	<100>	3,770 ± 30	$C_{44} = \rho v^2_{31}$	64.6 ± 1

[a] Reported value is based on only one successful measurement

Discussion

Composition and lattice parameters

The composition of the mineral from Novo Horizonte is close to YPO_4, but with significant amounts of other rare-earth elements from Sm to Lu. The total rare earth content amounts to a 24% replacement of Y ion in the YPO_4 lattice. Nevertheless, the lattice parameters of the mineral deviate only slightly from those of pure synthetic YPO_4. This can be analyzed/rationalized by studying the correlation between ionic radius and lattice parameters of the xenotimes.

Figure 2 shows the lattice parameters of the various pure rare-earth orthophosphates with xenotime structure, plotted as a function of the ionic radius of the rare-earth. It is seen that the lattice parameters of pure rare-earth orthophosphates with xenotime structure increase linearly with the ionic radius of the rare-earth. Based on the eight-coordinated ion radii (Shannon 1976) and Table 1, the mean eight-coordinated ion radius of the rare earth substitution is $R_{re} = 1.0263$ Å, close to that of Dy (1.0270 Å). The mean cation radius in *Y* sites is 1.0207 Å, which is only slightly larger than the Y ion radius $R_Y3+ = 1.019$ Å (Shannon 1976). This is consistent with lattice parameters that are only slightly larger than those for pure synthetic YPO_4. The lattice parameters of the mineral from the present work fall on the linear correlation with the rare earth ionic radius, in harmony with pure rare-earth orthophosphates with xenotime structure, Fig. 2.

Elastic constants

Measured and calculated constants of YPO_4 mineral

The elastic constants C_{11}, C_{33}, C_{44} and C_{66} could be measured reliably. The presence of microcracks in the mineral precluded direct measurement of the other constants. However, a correlation exists between elastic constants and compliance constants of xenotime, which can be used to extract the constants C_{12} and C_{13}.

Figure 3 shows the linear correlation between C_{11} and $1/S_{11}$, as well as that between C_{33} and $1/S_{33}$, for several synthetic xenotimes, for which elastic constants are available in the literature: $YVPO_4$ (Wang et al. 2000), $ErVO_4$ (Hirano et al. 2002), $ZrSiO_4$ (Ozkan et al. 1976), $LuPO_4$ and $LuAsO_4$ (Armbruster et al. 1974), and $YbPO_4$ (Nipko et al. 1996). The correlations are quite close, and can be expressed by the following equations:

$$\begin{aligned} C_{11} &= 1.144/S_{11} \\ C_{33} &= 1.192/S_{33}. \end{aligned} \tag{1}$$

From this correlation and using the measured C_{11} and C_{33}, the compliance constants were estimated. Using these values of S_{11} and S_{33}, along with C_{11} and C_{33}, the remaining constants C_{12} and C_{13} were calculated.

The resulting set of elastic constants is shown in Table 4 along with the literature data for a number of related isostructural compounds. The errors in Table 4

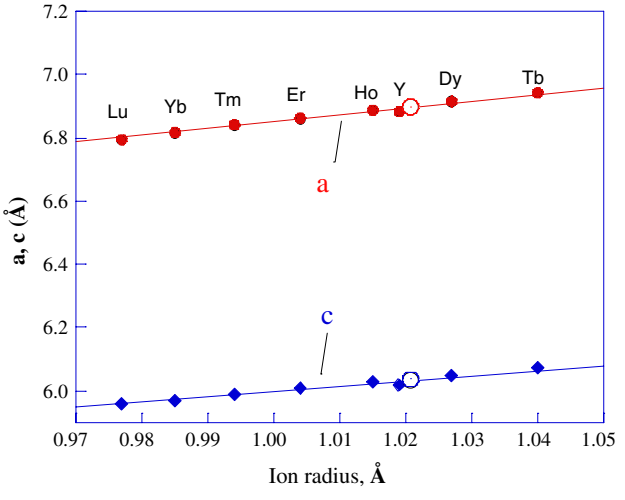

Fig. 2 Lattice parameters of the xenotime crystal used in this study (*open circles*) and of pure synthetic xenotimes (*filled symbols*, after Ushakov et al. 2001) plotted versus rare earth cation radius (Shannon 1976)

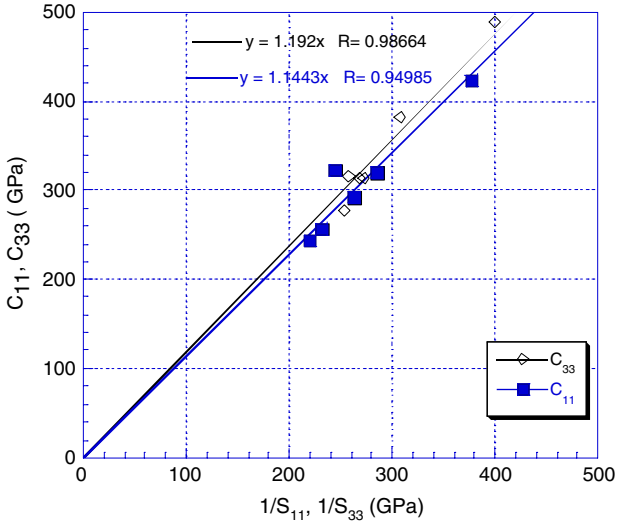

Fig. 3 Correlations between elastic constants C_{11} and C_{33} and the compliance constants S_{11} and S_{33} in synthetic xenotimes with known elastic constants: YVO_4, $ZrSiO_4$, $ErVO_4$, $LuPO_4$, $LuAsO_4$, and $YbPO_4$

Table 4 Room temperature elastic constants of natural Y xenotime and related compounds with xenotime structure

Elastic constant	Value (GPa)											
	YPO_4	$YbPO_4$	$LuPO_4$	$TmPO_4$	YVO_4	$TbVO_4$	$DyVO_4$		$HoVO_4$	$ErVO_4$	$NdVO_4$
C_{11}	220 ± 17	292	320	–	244.5	240	242		246.4	256.6	219[a]
C_{33}	332 ± 7	315	382	–	313.7	–	–		310.5	313	299
C_{44}	64.6 ± 1	87	84.6	67[b]	48.3	–	–		48.5	50.1	41.4
C_{66}	17.3 ± 1	35	21.7	16	16.2	13.1	15		16.07	17.7	–
C_{12}	55 ± 5[c]	22	36	–	48.9	55	50		88	53	–
C_{13}	86 ± 5[c]	–	115	–	81.1	–	–		–	79	–
Reference	Present work	Nipko et al. (1996)	Armbruster et al. (1974)	Harley and Manning (1998)	Wang et al. (2000)	Melcher (1976)	Melcher (1976) and Sandercock et al. (1972)		Goto et al. (1986)	Hirano et al. (2002)	Brown and Bolef (1979)

[a] At 9.9 K

[b] At 150 K

[c] Best fit to correlations (1)

represent the 95% confidence interval based on the measurement scatter. For the C_{66} constant, the extra error associated with the uncertainty of the sample orientation has been added to the statistical error. For C_{12} and C_{13} constants, the indicated errors represent the range of the best fit values based on the uncertainties of the other four elastic constants. The actual errors in the determination of C_{12} and C_{13}, however, depend on how well the correlation (1) is obeyed in the studied material.

Comparison to other crystals with xenotime structure

The C_{11} constant is somewhat lower than the value reported for synthetic YVO_4 (Wang et al. 2000), while C_{33} and C_{44} constants are notably higher (Table 4). The values of C_{66}, C_{12}, and C_{13} constants are close to the corresponding values reported for synthetic YVO_4.

It has been observed that the force constant of the bond between the rare earth and the nearest oxygen in the phosphates, arsenates, and vanadates of Lu and Y decreases monotonically with the increase of the RE-O distance (Armbruster 1976)[1]. This suggests a similar correlation for elastic constants. Figure 4 shows experimental C_{11} and C_{33} elastic constants for a number of rare earth orthophosphates and orthovanadates with xenotime structure plotted as a function of rare earth ion radius (ion radius after Shannon 1976). As the rare earth ion radius increases, C_{11} decreases monotonically for both phosphate and vanadate xenotimes. This trend suggests the expected value for the C_{11} constant of natural YPO_4 xenotime ~240 GPa, which is close to the value of 244.5 GPa of synthetic YVO_4 (Wang et al. 2000).

The measured C_{11} of the natural mineral is lower than expected value. This may be attributed to the effect of microcracks. Elastic modulus of porous solids can be described (Wanner 1998)

$$\frac{E}{E_0} = (1 - P)^{\eta}$$

where E_0 is the modulus of fully dense material, P is the porosity, and the exponent η depends on the shape of the pores and their orientation with respect to the loading direction (Wanner 1998). For randomly distributed spherical pores $\eta \approx 2$, while for closed microcracks aligned perpendicular to the loading direction $\eta \to \infty$. Assuming that the experimentally determined porosity of 2.4% is evenly distributed between (100) and

[1] See Appendix for a comment on the force constants.

(010) microcracks, and taking $E = 220$ GPa and $E_0 = 240$ GPa, we obtain $\eta \approx 7.2$. Wanner reported $\eta \approx 8.8$ for porous C/C composites, and $\eta \approx 25$ for plasma-sprayed spinel which had crack-like shaped pores with pronounced alignment normal to the load direction (Wanner 1998).

Unfortunately, the data for the C_{33} constant are rare, and the existing data appear more scattered, Fig. 4. The available data for vanadates indicate a weakly decreasing monotonic dependence of the C_{33} constant on the rare earth ion radius. The C_{33} reported for $YbPO_4$ (Nipko et al. 1996) fits the trend observed for vanadates. However, the reported C_{33} value for $LuPO_4$ and the measured value for natural xenotime are notably above this trend.

It is also interesting to compare the results with elastic constants calculated from the vibration frequencies (Armbruster 1976). The elastic constant C_{11} can be estimated from the corresponding frequency ν_{t1} of the translational mode (Armbruster 1976)

$$C_{11} = \frac{4\pi^2 \nu_{t1}^2 \mu}{c}.$$

Similarly, C_{33} can be estimated:

$$C_{33} = \frac{4\pi^2 \nu_{t3}^2 \mu c}{a^2},$$

where ν_{t1} and ν_{t3} are the respective translational frequencies, a and c are the lattice parameters, and μ is the reduced mass of Y^{3+} and $(PO_4)^{3-}$ ions. Substituting the frequencies $\nu_{t1} = 230$ cm^{-1} and $\nu_{t3} = 307$ cm^{-1} from Armbruster (1976), the lattice parameters $a = 6.88$ Å, $c = 6.02$ Å, and $\mu = 7.625\ 10^{-26}$ kg, we obtain $C_{33} = 324$ GPa and $C_{11} = 237$ GPa, in a good agreement with measured elastic constants.

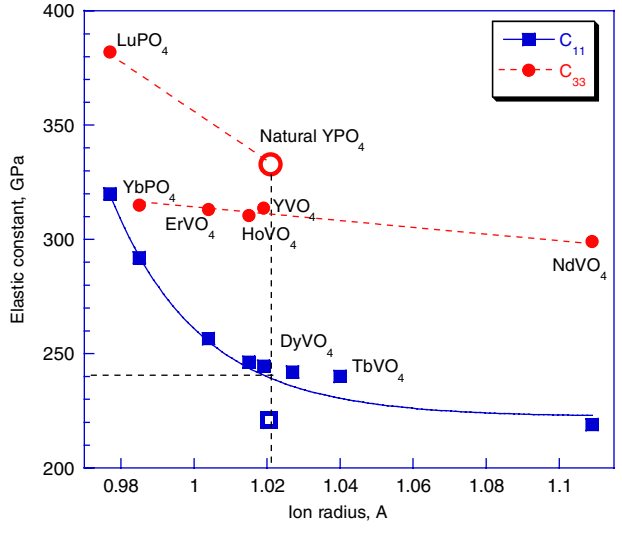

Fig. 4 Experimental C_{11} and C_{33} constants of rare earth orthophosphates and orthovanadates with xenotime structure (*filled symbols*, see references in Table 4) as a function of rare earth ion radius. *Open symbols* are the present data

Polycrystalline elastic constants

Based on the elastic constants in Table 4, the polycrystal averages can be computed. These are shown in Table 5. In addition to Voight and Reuss averages, the self-consistent estimates of random polycrystalline bulk, K, and shear, G, moduli (Berryman 2005) can be computed, as well as the corresponding Young's modulus E and Poisson ratio ν: $K = 132 \pm 9$ GPa, $G = 58 \pm 4$ GPa, $E = 152 \pm 9$ GPa, and $\nu = 0.31 \pm 0.01$ (the indicated uncertainties correspond to the uncertainties of the elastic constants in Table 4). The self-consistent estimate of random polycrystalline Young's modulus is in agreement with the experimental value $E = 152$ GPa for hot pressed polycrystalline xenotime (Kuo and Kriven 1995).

Conclusions

The composition, lattice parameters and elastic constants of natural single crystal YPO_4 xenotime from Novo Horizonte (Brazil) were determined using EPMA, XRD and pulse-echo technique. This mineral contains other rare-earths to the extent of a 24% substitution of the Y ion in the lattice. The relationship between the lattice parameters and the mean cation radius of the studied crystal was in a good agreement with the trends observed for pure synthetic orthophosphates with xenotime structure. The four elastic constants C_{11}, C_{33}, C_{44}, and C_{66} could be measured reliably. Due to the presence of {100} microcracks, the other two constants C_{12} and C_{13} were not measured, but were evaluated based on a comparison with other materials with xenotime structure. The experimentally measured elastic constants C_{11} in C_{33} are in a good

Table 5 Polycrystal elastic constants computed from data in Table 4

	Voight	Reuss	Random effective (Berryman 2005)
Young's modulus	170	120	152
Bulk modulus	136	129	132
Shear modulus	66	45	58
Poisson ratio	0.29	0.34	0.31

agreement with those calculated from the literature data on the vibrational frequencies of synthetic YPO_4.

Acknowledgment This work was supported by the Air Force Research Laboratory (AFRL), Materials and Manufacturing Directorate, under Contract No. F33615-01-C-5214. The authors would like to thank Mr. Marlin Cook (UES, Inc.) for his help with specimen preparation.

Appendix: interionic force constants and bond energies

The xenotime lattice of YPO_4 consists of PO_4 tetrahedra and eight-coordinated Y ions, with four YPO_4 molecules per unit cell (Ni et al. 1995). Of the eight Y–O bonds, the four shorter bonds (2.309 Å) extend essentially laterally nearly parallel to (001) plane. The other four are longer (2.382 Å) and are links in the ionic chains that extend along the [001] (Ni et al. 1995). The bond energy can be estimated using the empirical relationship between the bond energy and bond length (Ziółkowski 1985; Ziółkowski and Dziembaj 1985). This produces 263 and 226 kJ per mole of the equivalent bonds (4.37×10^{-19} and 3.75×10^{-19} J per bond) for the shorter and longer Y–O bonds, respectively. The energy of the P–O bonds is higher (352 kJ/mol or 5.84×10^{-19} J per P–O bond). Although this difference is not as pronounced as between Ca–O and W–O bonds in scheelite (Neiman 1996), the mean P–O distances remain nearly unchanged for all rare-earth orthophosphates from La to Lu (Ni et al. 1995). Furthermore, although there appears to be no high pressure data for xenotime, PO_4 tetrahedra in aluminum, boron, and lead orthophosphates are rigid and undergo little structural change with pressure (Haines et al. 2003; Angel et al. 2001). For this analysis, it can be assumed that at least at room temperature the PO_4 tetrahedra are incompressible, and the elastic properties of xenotime are due to the compressibility of the Y–O bonds alone.

The force constants of rare earth–oxygen bonds for a number of compounds with xenotime structure, including synthetic YPO_4, have been evaluated by Armbruster (1976) from the frequencies of the translational infrared vibrations of the RE ions against the tetrahedral ions using a simple central force constant model. However, we suggest that the equations used by Armbruster (1976) to extract the force constants contain an error. Retaining the notations used by Armbruster (1976), the correct set of equations is:

$$\begin{aligned} 4\pi^2 \nu_{\mathrm{trans}}^2(A_{2u}) &= [4f_n \cos^2(\theta_n/2) + 4f_{nn}\cos^2(\theta_{nn}/2)]/\mu \\ 4\pi^2 \nu_{\mathrm{trans}}^2(E_u) &= [2f_n \sin^2(\theta_n/2) + 2f_{nn}\sin^2(\theta_{nn}/2)]/\mu, \end{aligned} \tag{A1}$$

where μ is the reduced mass of the rare earth and the tetrahedral ion, f_n and f_{nn} are the force constants for the shorter and longer RE–O bonds, respectively, and the angles θ_n and θ_{nn} are the angles between these bonds and the c-axis of the lattice. Substituting the frequencies $\nu_{\mathrm{trans}}(A_{2u}) = 307\ \mathrm{cm}^{-1}$ and $\nu_{\mathrm{trans}}(E_u) = 230\ \mathrm{cm}^{-1}$ (Armbruster 1976) and the angles $\theta_n = 76.27°$ and $\theta_{nn} = 30.36°$ calculated based on the atomic coordinates of pure YPO_4 (Ni et al. 1995), we obtain $f_n = 85$ J/m and $f_{nn} = 54$ J/m. These constants are not only somewhat higher than those reported by Armbruster (1976) (41 and 63 J/m, respectively), but, more importantly, the shortest bond now has a higher force constant, more in line with the respective bond energies calculated above. Furthermore, according to Ziółkowski (1985) and Ziółkowski and Dziembaj (1985) the bond energy U is inversely proportional to the effective bond length:

$$U = \frac{A}{R - R_0}, \tag{A2}$$

where R is the bond length and R_0 is the sum of the effective radii of the two ions (Ziółkowski 1985; Ziółkowski and Dziembaj 1985). The force constant then can be obtained as

$$f \sim \frac{\partial^2 U}{\partial R^2} \sim \frac{A}{(R - R_0)^3} \sim U^3 \tag{A3}$$

and the ratio between the two force constants f_n/f_{nn} should equal $(U_n/U_{nn})^3$. Indeed, $f_n/f_{nn} = 1.574$ and $(U_n/U_{nn})^3 = 1.576$.

References

Aldred AT (1984) Cell volumes of APO_4, AVO_4, and $ANbO_4$ compounds, where A = Sc, Y, La–Lu. Acta Crystallograph B40:569–574

Andrehs G, Heinrich W (1998) Experimental determination of REE distributions between monazite and xenotime: potential for temperature-calibrated geochronology. Chem Geol 149:83–96

Angel RJ, Bismayer U, Marshall WG (2001) Renormalization of the phase transition in lead phosphate, $Pb_3(PO_4)_2$, by high pressure. Struct J Phys Condens Matter 13:5353–5364

Armbruster A (1976) Infrared reflection studies on the phosphates, arsenates, and vanadates of Lutetium and Yttrium. J Phys Chem Solids 37:321–327

Armbruster A, Thoma R, Wehrle H (1974) Measurement of the elastic constants of $LuAsO_4$ and $LuPO_4$ by Brillouin scattering and determination of Debye temperatures. Phys Stat Solid A 24:K71–K73

Berryman JG (2005) Bounds and self-consistent estimates for elastic constants of random polycrystals with hexagonal,

trigonal, and tetragonal symmetries. J Mech Phys Solid 53:2141–2173
Blundy JD, Wood BJ (2002) Prediction of crystal–melt partition coefficients from elastic moduli. Nature 372:452–454
Blundy JD, Wood BJ (2003) Partitioning of trace elements between crystals and melts Earth and Planetary. Sci Lett 210:383–397
Brown J, Bolef DI (1979) Magnetoelastic interactions in $NdVO_4$. Finite strain and rotational effects. Phys Rev B Condens Matter 19:5847–5857
Davis JB, Lofvander JPA, Evans AG, Bischoff E, Emiliani ML (1993) Fiber coating concepts for brittle matrix composites. J Am Ceram Soc 76:1249–1257
Davis JB, Marshall DB, Housley RM, Morgan PED (1998) Machinable ceramics containing rare-earth phosphates. J Am Ceram Soc 81:2169–2175
Finch RJ, Hanchar JM, Hoskin PWO, Burns PC (2001) Rare-earth elements in synthetic zircon: part 2. A single-crystal X-ray study of xenotime substitution. Am Mineral 86:681–689
Goto T, Tamaki A, Fujimura T (1986) Quadrupolar response and rotational invariance of single ground state system: HoVO4. J Phys Soc Jpn 55:1613–1623
Gratz R, Heinrich W (1997) Monazite–xenotime thermobarometry: experimental calibration of the miscibility gap in the binary system $CePO_4$–YPO_4. Am Mineral 82:772–780
Gratz R, Heinrich W (1998) Monazite–xenotime thermometry. III. Experimental calibration of the partitioning of gadolinium between monazite and xenotime. Eur J Mineral 10:579–588
Haines J, Chateau C, Léger JM, Bogicevic C, Hull S, Klug DD, Tse JS (2003) Collapsing cristobalitelike structures in silica analogues at high pressure Phys Rev Lett 91:015503/1–4
Harley RT, Manning DI (1978) Jahn–Teller induced elastic constant changes in $TmPO_4$. J Phys C Solid State Phys 11:L633–L636
Hirano Y, Guedes I, Grimsditch M, Loong CK, Wakabayashi N, Boatner LA (2002) Brillouin-scattering study of the elastic constants of $ErVO_4$. J Am Ceram Soc 85:1001–1003
Keller KA, Mah T, Parthasarathy TA, Boakye EE, Mogilevsky P, Cinibulk MK (2003) Effectiveness of monazite coatings in oxide/oxide composites in extending life after long-term exposure at high-temperature. J Am Ceram Soc 86:325–332
Kerans RJ, Hay RS, Parthasarathy TA, Cinibulk MK (2002) Interface design for oxidation-resistant ceramic composites. J Am Ceram Soc 85:2599–2632
Kuo DH, Kriven WM (1995) Characterization of yttrium phosphate and yttrium phosphate/yttrium aluminate laminate. J Am Ceram Soc 78:3121–3124
Marshall DB, Morgan PED, Houley RM, Cheung JT (1998) High-temperature stability of the Al_2O_3–$LaPO_4$ system. J Am Ceram Soc 81:951–956
McSkimin HJ (1964) Ultrasonic methods for measuring the mechanical properties of liquids and solids, In: Mason WP (ed) Physical acoustics. Academic, New York, vol 1, Pt A, pp 271–334
Melcher RL (1976) The anomalous elastic properties of materials undergoing cooperative Jahn–Teller phase transitions. In: Mason WP, Thurston RN (eds) Physical acoustics. Academic, New York, pp 1–77
Morgan PED, Marshall DB (1993) Functional interfaces for oxide/oxide composites. Mat Sci Eng A 162:15–25
Morgan PED, Marshall DB (1995) Ceramic composites of monazite and alumina. J Am Ceram Soc 78:1553–1563
Morgan PED, Marshall DB, Housley RM (1995) High temperature stability of monazite–alumina composites. J Mat Sci Eng A 195:215–222
Neiman AY (1996) Cooperative transport in oxides: diffusion and migration processes involving Mo(VI), W(VI), V(V) and Nb(V). Solid State Ionics 83:263–273
Ni Y, Hughes JM, Mariano AN (1995) Crystal chemistry of the monazite and xenotime structures. Am Mineral 80:21–26
Nipko J, Grimsditch M, Loong C-K, Kern S, Abraham MM, Boatner LA (1996) Elastic constant anomalies in $YbPO_4$. Phys Rev B Condens Matter 53:2286–2290
Ozkan H, Cartz L, Jamieson JC (1976) Elastic constants of nonmetamict zirconium silicate. J Appl Phys 47:4772–4779
Pile JM, Spear FS, Rudnick RL, McDonough WFM (2001) Monazite–xenotime–garnet equilibrium in metapelites and a new monazite–garnet thermometer. J Petrol 42:2083–2107
Roberts WL, Campbell TJ, Rapp GR, Wilson WE (1990) Encyclopedia of Minerals, 2nd edn. Van Nostrand Reinhold, New York
Sandercock JR, Palmer SB, Elliot RJ, Hayes W, Smith SRP, Young AP (1972) Brillouin scattering, ultrasonic and theoretical studies of acoustic anomalies in crystals showing Jahn–Teller phase transitions. J Phys C Solid State Phys 5:3126–3146
Seydoux-Guillaume A-M, Wirth R, Heinrich W, Montel JM (2002) Experimental determination of the Th partitioning between monazite and xenotime using analytical electron microscopy and X-ray diffraction Rietveld analysis. Eur J Mineral 14:869–878
Shannon RD (1976) Revised effective ionic radii and systematic studies of interatomic distance in halides and chalcogenides. Acta Crystallogr A 32:751–767
Tabor D (1970) The hardness of solids. Rev Phys Technol 1:145–179
Ushakov SV, Helean KB, Navrotsky A, Boatner LA (2001) Thermochemistry of rare-earth orthophosphates. J Mater Res 16:2623–2633
Wang R, Li F, Wu X, Yang H (2000) Ultrasonic study on Nd:YVO_4 crystals. Chin J Lasers A 275:449–454
Wanner A (1998) Elastic modulus measurements of extremely porous ceramic materials by ultrasonic phase spectroscopy. Mat Sci Eng A 248:35–43
Wood BJ, Blundy JD (1997) A predictive model for rare earth element partitioning between clinopyroxene and anhydrous silicate melt. Contrib Mineral Petrol 129:166–181
Ziółkowski J (1985) New relationship between ionic radii, bond length, and bond strength. J Solid State Chem 57:269–290
Ziółkowski J, Dziembaj L (1985) Empirical relationship between individual cation–oxygen bond length and bond energy in crystals and in molecules. J Solid State Chem 57:291–299